

Report from Team Horizon on the Challenge from Guru Dhwani

C.V. Krishnamurthy¹, Amogh Waghmare², Amrit³, Arjun R⁴,
Nidhi Biswas⁵, Annirudha⁶, Vivan Bhatt⁷, and Aditya Kumar⁸

¹Indian Institute of technology Madras IITM), Department of
Physics Mentor)

^{2 3 5 6 7 8}IITM, Department of Physics

⁴IITM, Department of Electrical Engineering

September 2021-January 2022

bstract

1 Introduction to the team

We are a group of highly motivated undergraduate students under the guidance of Prof. C.V Krishnamurthy, who came together under the aegis of Horizon, the astronomy and physics club at IIT Madras. We entered this competition with the twin objectives of exploring the domain of radio astronomy, and acquiring hands-on experience with the bleeding edge of research in antenna theory.

In this report, we document our findings and make our suggestions for a radio antenna suitable for detecting Jovian decametric radiations while satisfying the given constraints.

2 Theory

2.1 Jovian Radiation

The interaction between Io and Jupiter enhances Jupiter's emission of decameter radio waves – at certain points in Io's orbit, our chances of receiving radio waves is much more probable. These Io-related sources are called Io-A, Io-B, Io-C and Io-D based upon our likelihood of observing them, and are often represented via CML (Central Meridian Longitude) vs Io phase plots. In these plots, CML is defined by the longitude of Jupiter facing the Earth at a given time, and Io phase is the angle of IO with respect to superior geocentric conjunction.

Io-related storms	Characteristics
Io-A	Right hand polarized and mostly long bursts
Io-B	Right hand polarized and mostly short bursts
Io-C	Left Hand polarized, long and short bursts height

Table 1: Jovian Radio bursts

[The Jovian Decametric Radio Emission \(nasa.gov\)](#)

Jovian decametric emission was discovered in 1955 by BF Burke and KL Franklin at 22 MHz, and has since been found to have an upper cuto frequency of 39.5 MHz, and with the intensity peak at 8 MHz. It can be detected from ground-based stations from the upper cuto frequency down to the cuto frequency of the terrestrial ionosphere, which is generally around 5-10 MHz.

Most of the radio waves from Jupiter are polarized, indicating the existence of a magnetic field. The decametric emission occurs in episodes called “storms”, which can last between a few minutes and a few hours. During a storm, we can receive two types of bursts. The Long Bursts vary slowly in intensity with time, generally lasting for a few seconds, with an instantaneous bandwidth of a few MHz. The Short Bursts are very short in duration, with an instantaneous bandwidth of a few KHz to a few tens of KHz, drifting downwards at a rate of typically 20 MHz/s. They arrive at a rate of a few to several hundred bursts per second, and sometimes, both types of bursts can be detected simultaneously. We include a table with regards to the polarization of Jovian radio bursts. The mechanism of emission of these radio waves is commonly studied via the cyclotron-maser theory, and the emission from several Io storms analysed by using the complete Stokes Polarimetry yielded the following major conclusions [2],[3]

1. The polarization fraction m is quite large
2. The polarization is always elliptical. The absolute values of the axial ratio $|\nu|$ are generally less than 0.6
3. Io-A storms show more circular polarization than Io-B storms.
4. Almost all events show nearly constant polarization as a function of frequency and time, even in the storms which last for a few hours

3 A design based on the Log Periodic Antenna

3.1 Log periodic antenna

Log periodic antennas in their present form came about from the work of D. E. Isbell at the University of Illinois in the late 1950s. These antenna are directional and have constant characteristics over a wide range of frequencies.

Log periodic antennas are designed in such a way that their performance is a periodic function of the log of frequency. This enables them to have a substantial bandwidth and a stable radiation pattern. When dipoles are used as radiating elements, a good gain and a large beamwidth is also achieved.

Apart from these electromagnetic advantages, they can be built using cheaply available metal tubes. Furthermore, being wire antennas, they do not yield to winds even though they span large areas removing the need for any costly mechanical support systems. They have been used to study various astronomical phenomena like solar corona emissions and various other phenomenon before [4],[5],[6].

Their structure is completely specified by three parameters τ , σ [7]

$$\tau = \frac{R_{n+1}}{R_n} = \frac{D_{n+1}}{D_n} = \frac{L_{n+1}}{L_n}$$

$$\tan(\alpha) = \frac{1 - \tau}{4\sigma} = \frac{D_n}{2L_n}$$

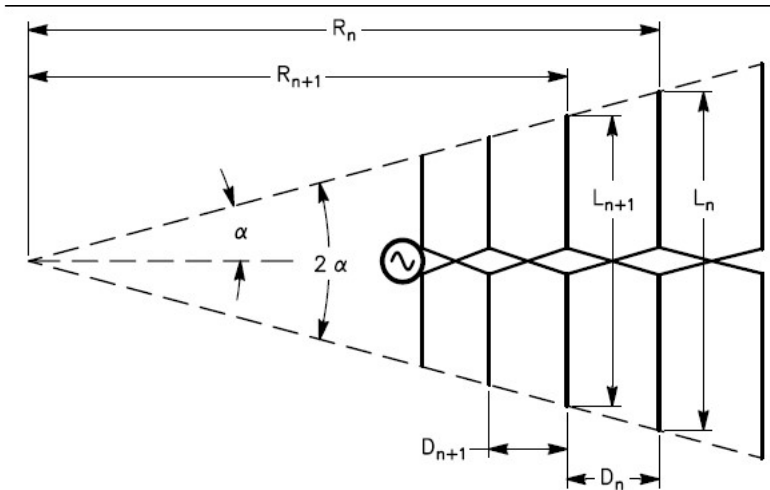


Figure 1: Log periodic dipole antenna (ARRL Antenna book 21st ed.)

We have used an [online calculator](#) to find the design specifications and used 4Nec2 to modify and simulate the design.

Two such units which were discussed in the above section will be co-located orthogonally so that the antenna can detect radiation with circular polarization. These units will have separate receivers.

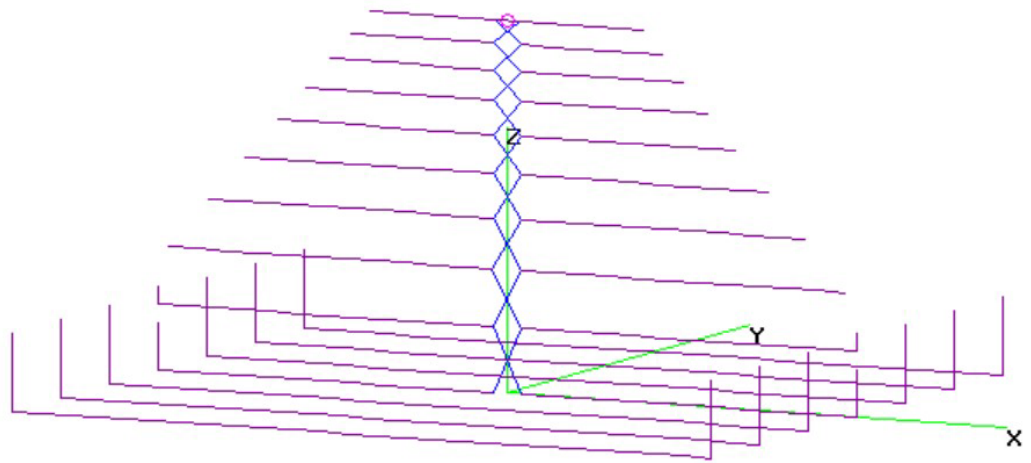


Figure 2: Structure of a single unit in 4NEC2 (purple lines are wires, the blue crisscrossed line represents a transmission line) z axis is normal to the ground

3.2 Design

We have designed our antenna such that best reception occurs from 18-24 MHz, a range where radio emissions from Jupiter are easily detectable [8]. We used $\tau = 0.878$ and $\sigma = 0.07$ for our design

Table 2: Lengths of dipole elements

l1	8.817m
l2	7.742
l3	6.797m
l4	5.978m
l5	5.240m
l6	4.602m
l7	4.4039
l8	3.547
l9	3.114
l10	2.734

Table 3: distances between dipoles

d1	1.234m
d2	1.084m
d3	0.952m
d4	0.836m
d5	0.734m
d6	0.644m
d7	0.566m
d8	0.497m
d9	0.436m

Input impedance of the antenna is designed to be 200 ohms and a 4:1 current balun can be used to convert this to 50 ohms so that a commercially available coaxial cable (RG223) can be used [8]. We plan to place this balun in one of the booms. The inner conductor of the coaxial cable is connected to one of the booms and the outer to the other at the top of the structure and the cable is routed through one of the booms to the receiver unit.

Transmission line impedance comes out to be 321.4 ohm, The boom acts as a circular rectangular transmission line with insulating spacers to provide the impedance required. This can be made using a commercially available square aluminium pipes with sufficient width to allow the passage of the coaxial cable and the housing of the balun. The impedance of such a transmission line is given by

$$Z_o = 120 \cosh^{-1} \frac{D}{1.18w}$$

[7] where w is the width of the square and D is the center to center spacing between the tube. We use the methods described in the ARRL antenna book to connect the dipoles to the boom. To accommodate the coaxial cable, we choose d to be 20mm with a thickness of 5mm(the coaxial cable has diameter 5.4mm) from this we get D to be 173mm

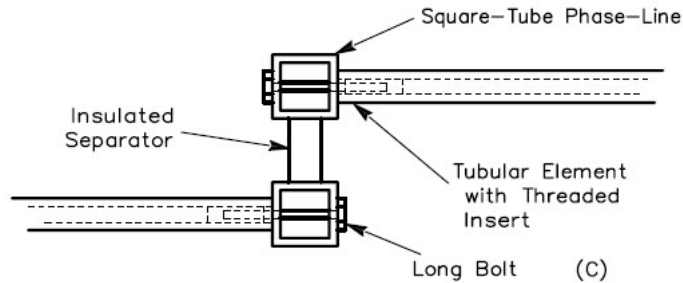


Figure 3: Construction of boom and attachment of dipoles to the boom (ARRL antenna book 21st.ed)

The boom also provides mechanical support to the antenna.

Since two of the longest dipole elements have lengths larger than 7m, they were bent to meet the size constraints. We plan to make these dipoles using commercially available aluminium tubes of 13mm diameter following the example of [4]

The reflector is made up of wires of length 10 m which are laid 1m apart and are bent at their ends (3.5m from the middle), these act as reflectors for most of the frequencies in the band of 17-37 MHz. These will also be made using the same aluminium tubes.

3.3 Support structures

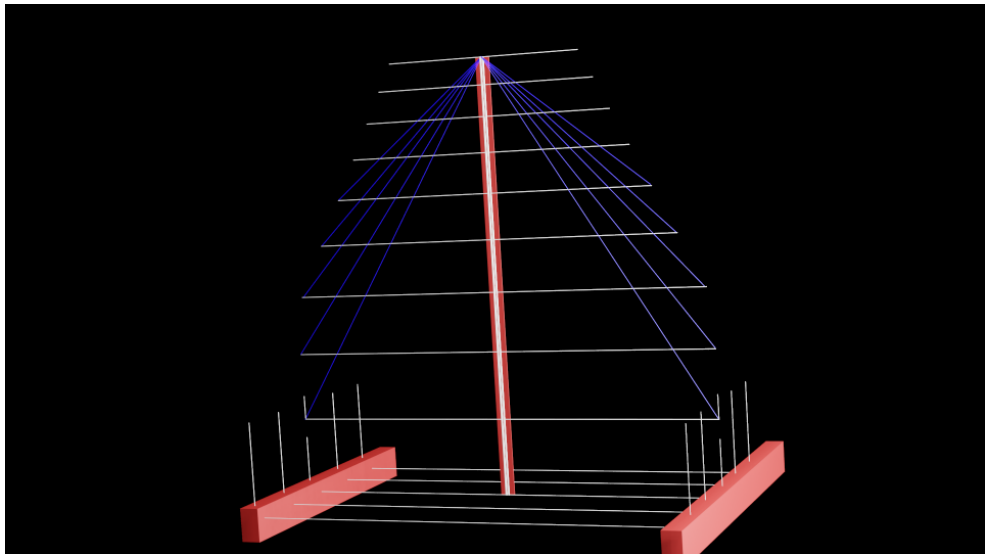


Figure 4: 3D model with support structure

The beam of the antenna as of now would be vertically positioned. Due to the long lengths of most of the elements of the antenna, we have to use support structures which will prevent sagging caused due to their own weights, winds and other natural phenomenon. For this, we provide the diagram as a rough sketch of the support system.

The wooden beam provides support to the central boom, the nylon strings support the dipoles and the wooden casing on the ground supports the bent portions of the reflector.

Lightning protection devices will be directly installed on the antenna to protect the antenna from over-voltage damage.

Severe weather events can affect satellite signals caused by rain and atmospheric moisture. In order to ensure continuous signal availability, even in the case of failure of a part of the transmission chain, routes are designed redundantly. If a section of the route fails, a backup can take over the signal transmission of the failed part. Since backup equipment is only required in the rare case of a primary path failure, an effective solution could be to implement one redundant antenna for a set of antennas to reduce the cost. A motorized steerable backup antenna can be employed to restore failure of 1 or more fixed (non-steerable) antennas in a facility. ([From antenna to receiver](#))

3.4 Innovative features and challenges faced

A significant issue with designing an antenna for detecting emissions centered at 20MHz is its size. An unmodified log periodic antenna in this regime (for a frequency of 17-37MHz) would have a boom length of approximately 17m and have dipole elements as long as 8m.

The antenna is designed such that only some of the dipoles receive radiation of a given frequency effectively, while dipoles longer than these act as reflectors which provide a good FB ratio at higher frequencies. The FB ratio falls off at the lower edges of the band, where most of the frequencies of interest (18-24MHz) lie in this case due to size constraints on the antenna. This necessitates the use of reflector elements.

Raja et.al [4] have reported that when two such antennas are co-located orthogonally to detect circularly polarized radiation, they interfere with each other's performance resulting in poor isolation and an inability to characterize the polarization of the incoming radiation.

The placement of the balun in one of the booms may affect antenna performance. A design that does not use a balun needs to have a shorted transmission line stub attached at the end where the longest dipole element is present. This stub has a length of about 2m and will violate the 7-meter size constraint.

We reduced τ and σ , which reduced the boom length and the directivity. To reduce the size of the dipole elements, we made use of the well-known fact that the current at the ends of a dipole antenna is nearly zero, which enabled us to bend the two longest dipole elements without affecting the gain or the impedance matching of our antenna. We modeled several bent configurations before arriving at one that did not significantly degrade the impedance matching at lower frequencies.

We attempted to improve the FB ratio in the range of frequencies of interest(18-24MHz) by making reflectors out of 10m wires, bending them at their ends to satisfy the size constraints. These act as effective reflectors for the 2nd longest dipole and upwards since the longest one is at the same level as them. Since the longest dipole does not radiate well at these frequencies, and simulations provided a good FB ratio, we did not find it necessary to place the antenna at a height above the reflectors. We also tried different values for the spacing of these reflectors and found that 6 of these provided a good FB ratio and did not degrade the impedance matching significantly.

3.5 Results

3.5.1 Impedance matching and bandwidth

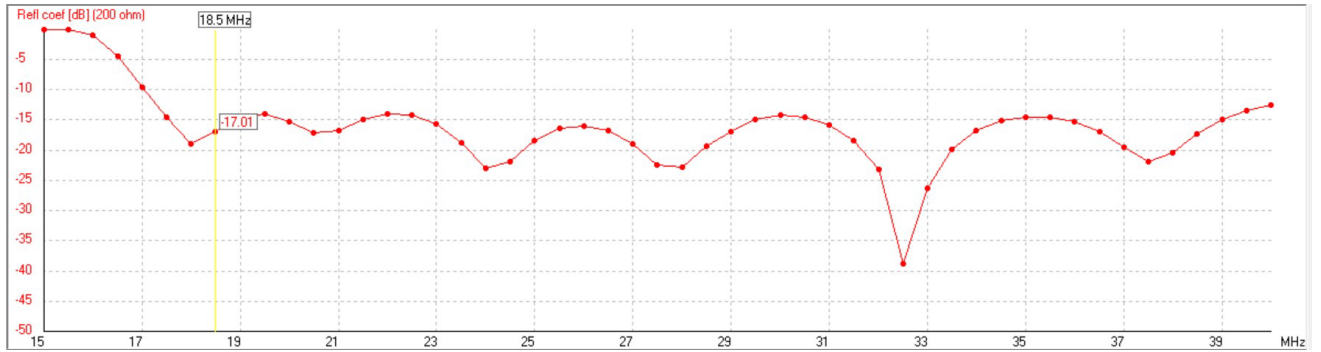


Figure 5: S11 plot for the designed antenna when fed using a 200 ohms coaxial cable

The simulations reveal an excellent bandwidth(S11 below -10dB) of about 27.5 MHz(17.5-45MHz). Apart from this, the S11 is below or very close to -15dB in the region of interest.

3.5.2 Radiation pattern and beamwidth

The radiation patterns were stable and had a single lobe in the forward direction with a maximum gain of about 7 dB and a 3dB beamwidth of at least 60 degrees throughout the band and 70 degrees in the region of interest. We managed to achieve a FB ratio above 25dB in the range of 19-23MHz.

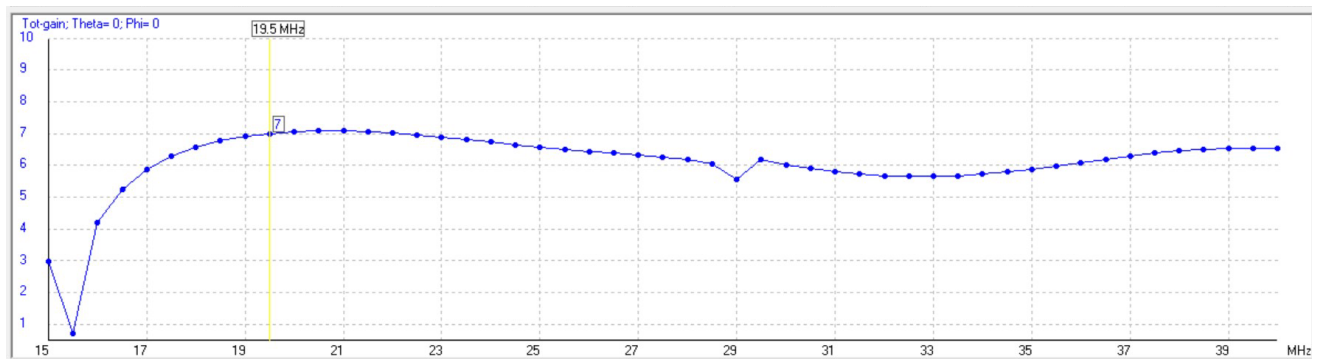


Figure 6: Maximum gain of the antenna

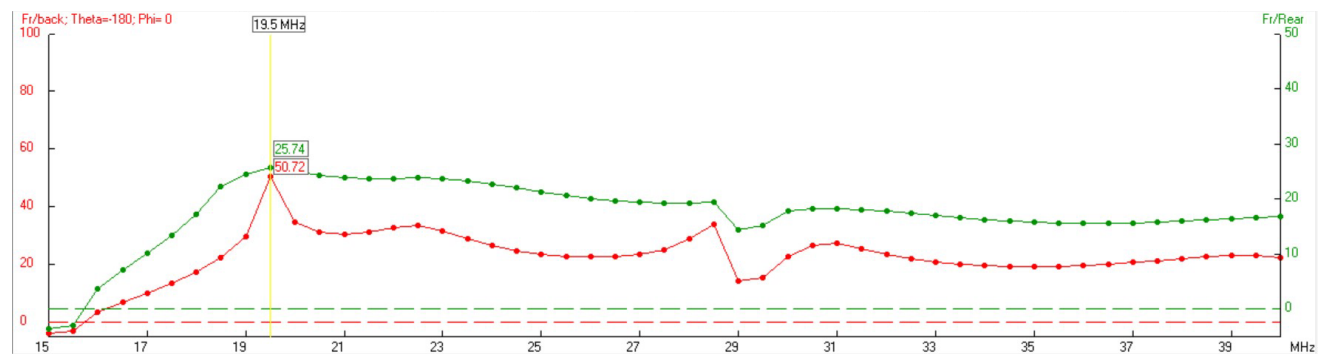


Figure 7: Front to back ratio

3.5.3 Radiation pattern at various frequencies

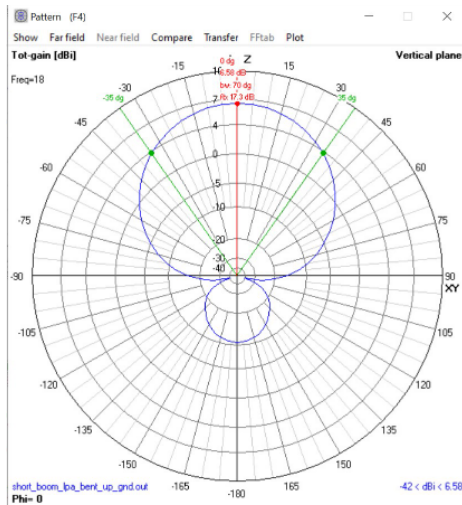


Figure 8: 18 MHz

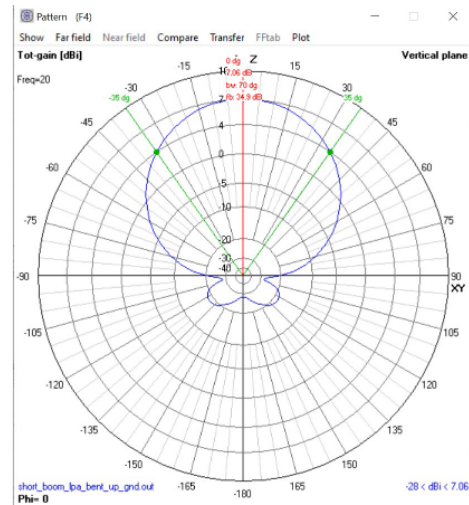


Figure 9: 20MHz

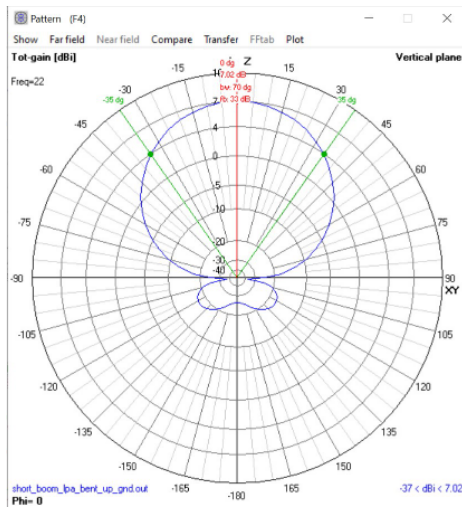


Figure 10: 22MHz

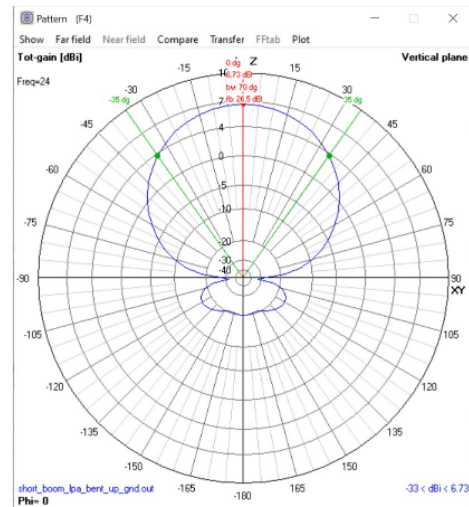


Figure 11: 24MHz

4 Looking at Jupiter

4.1 Motion of Jupiter

Jupiter just like Sun, rises in the east and sets in the west when seen from Chennai. The azimuth of the ascending point is around east with a deviation of 20 degrees and the descending point is around west with a deviation of 20 degrees.

To observe the radio bursts from Jupiter, the line of incident radiation should mostly be in the region of maximum gain of our antenna to ensure accurate results.

The angle of altitude of Jupiter, maximum elevation from horizon and other parameters have been noted down for the next 5 years in a time step of 1 month to properly analyse the motion of Jupiter.

The half beam width at half maximum for our antenna comes out to be 56 degrees at an azimuth of 90 degrees. From this, one can infer that the angle of altitude for Jupiter has to lie above 34 degrees for accurate recordings by the antenna. This observation time has been calculated using [Stellarium](#). The below table for a year is an example of our data, and here is the link for our full data [data](#).

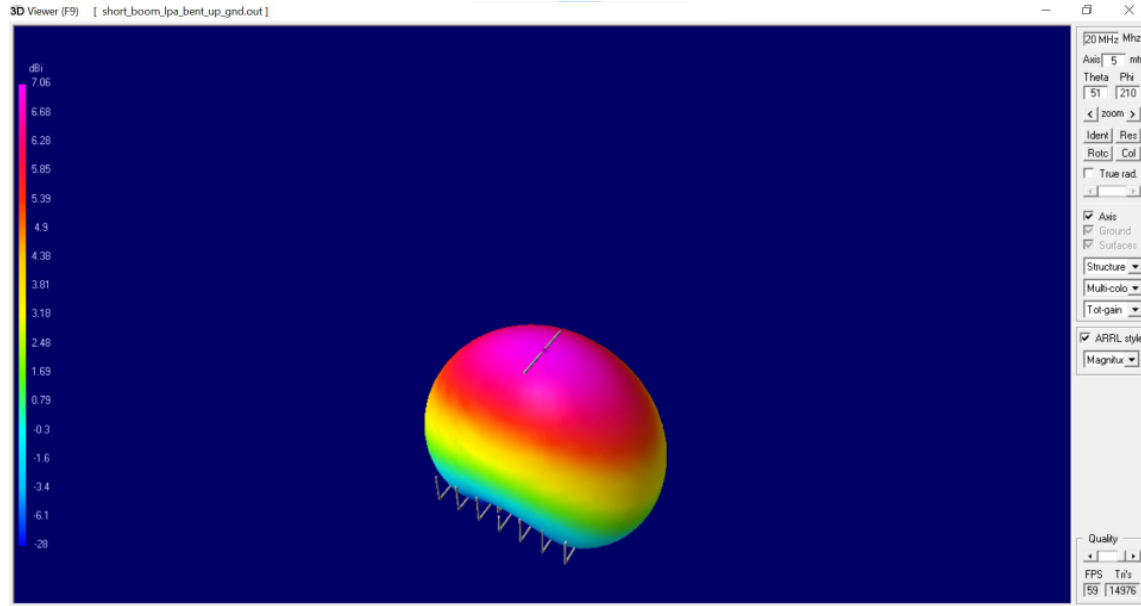


Figure 12: 3D radiation pattern

Table 4: Observation of Jupiter using Stellarium.

D	ME(degrees)	t1	t2	T
15-16/1/2022	65°	11:30	18:20	6hrs 50min
15-16/2/2022	68° 30'	9:50	16:45	6hrs 55min
15-16/3/2022	71° 10'	8:18	15:24	7hrs 06min
15-16/4/2022	74°	6:42	13:53	7hrs 11min
15-16/5/2022	76° 22'	5:04	12:21	7hrs 17min
15-16/6/2022	78° 10'	3:18	10:39	7hrs 21min
15-16/7/2022	79° 06'	1:29	8:52	7hrs 23min
15-16/8/2022	78° 52'	23:27	6:50	7hrs 23min
15-16/9/2022	77° 38'	21:11	4:31	7hrs 20 min
15-16/10/2022	76° 03'	19:01	2:18	7hrs 17min
15-16/11/2022	75° 12'	16:52	00:06	7hrs 14min
15-16/12/2022	75° 36'	14:55	22:11	7hrs 17min

D - date

ME - Maximum angle of elevation

t1 - time when jupiter is ascending the altitude of 34 degrees

t2 - time when jupiter is descending the altitude of 34 degrees

4.2 Placing the Antennas

The antenna will be placed almost along the North-South direction, and can be rotated using the azimuth mount (discussed further in the section of Scope for Improvements)

When two antennas are co-located as discussed in the design subsection, the following can be done for properly analyzing the two polarizations of the Jovian radiation -

Let the origin of a spherical polar coordinate system be situated at the antenna. Consider a specific direction of incidence of radiation. This direction can be described by a certain theta and a certain phi. For this theta and phi, the gains for the two antennas (of orthogonal polarizations) would not be equal in general.

However, since the signals are separately received, we know the gains with which each antenna has collected the incident radiation since we know the position of Jupiter. We can proceed to recover the correct signal.

5 Receiver System

5.1 Various Components of the Receiver System

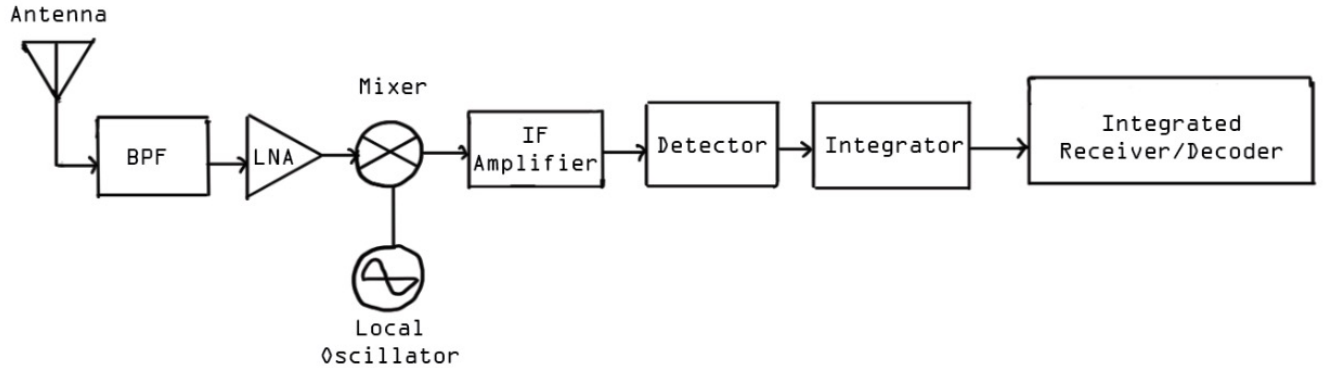


Figure 13: Block diagram for the receiver system from [9]

The antenna is connected to a band pass filter (BPF) to allow only a range of frequency from 18 - 30 MHz[8]. This is done to prevent noise from radiations outside this range. Then BPF is followed by a low noise amplifier (LNA). The LNA is connected to amplify the signals as they are usually weak. The BPF is placed before LNA because otherwise the radio frequency interference outside the band can lead to nonlinearity in the LNA. The coaxial cable connects the BPF to a LNA.

Followed by this is an IF amplifier in which we multiply a frequency of our choice using a mixer thus changing the frequency of the signal[9]. An Integrator is also connected in the circuit. It integrates the input of a large number of trials to give an output. This reduces the noise in the frequency range. The next step is to connect the LNA to IRD.

We could also use a Software Defined Radio (SDR) which is programmable and supports various wireless technologies without the need to update hardware. The biggest advantage of this software is that it is able to measure both short radio bursts and long radio bursts. It is also advantageous as it is easily upgradable, reconfigurable and has low maintenance cost. (See - [Advantages and disadvantages of SDR](#).)

5.2 Cable

If the antenna has transmission paths of less than 100 meters from LNA to IRD, transmission over coaxial cable introduces minimal losses and is typically acceptable for cost reasons. For larger cabling distances, where bigger line losses over coax would result. Radio frequency over fibre transmission has major advantages and should be used. In such a scenario, radio waves are converted into light pulses and then transmitted over a fiber optic cable. This ensures very low signal loss, and the resulting system is lightweight, flexible and requires low maintenance.(See - [From antenna to receiver](#))

5.3 Housing of the various components

This idea is borrowed from the Faraday Cage of GMRT telescope.
A caging of metal doors and wire meshing on windows can be in the building that houses the equipment to protect it from lightning. The wire spacing must be less than 1/5 of the minimum operating wavelength of the antenna, or lower.

6 Scope for Improvement

6.1 Azimuthal Mount

The trajectory of Jupiter has to be calculated using our position on earth as origin. It would be convenient to do this in spherical coordinates. The gain pattern in 4nec2 should be exported and the gain values at a given altitude and azimuth should be noted down.

Now using computational techniques, we can get the gain corresponding to Jupiter's position in the sky. The above computation will help us in calibrating the azimuth mount, allowing us to position the antenna such that Jupiter lies in the region with maximum gain.

Let the origin of a spherical polar coordinate system be situated at the antenna. Consider a specific direction of incidence of radiation. This direction can be described by a certain theta and a certain phi. For this theta and phi, the gains for the two antennas (of orthogonal polarization) would not be equal in general. However, since the signals are separately received, we know the gains with which each antenna has collected the incident radiation since we know Jupiter's position. We can proceed to recover the correct signal.

7 Appendix

We mention some other designs which were rejected due to certain deficiencies in their design and/or output.

7.1 Magneto dielectric antenna

We attempted to simulate a magneto dielectric antenna as presented by Luk and Wang [10] in 4Nec2. The antenna did not satisfy the size constraints but its bandwidth of 1.2GHz(1.8 -3GHz) and a stable gain of about 15dB. Since 4Nec2 does not allow modeling open sheets, we had to replace the design given in the paper with a wire mesh design scaled to a center frequency of 20MHz from 2.5GHz. The mesh design could not replicate the microstrip line made out of sheets in the original design, and making large enough mesh for the ground plane was not feasible computationally. We tried to make the design without these features by using 4Nec2 ground and feeding the antenna directly at the point where the microstrip line terminated in the original design. We could not proceed with the design due to largely inaccurate simulations.

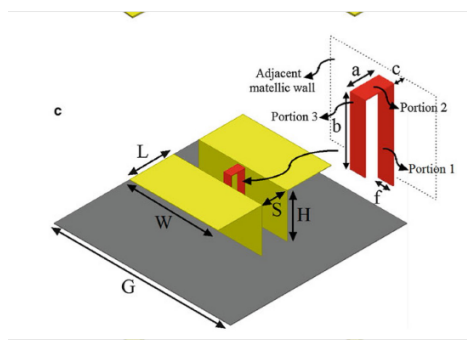


Figure 14: Original design

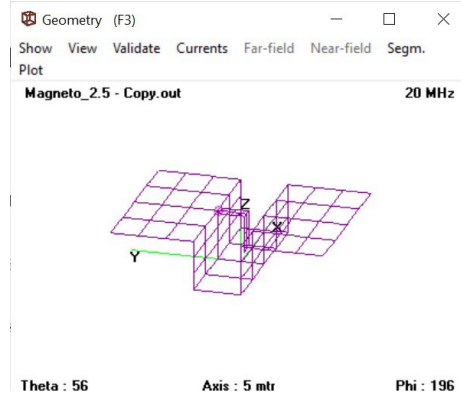


Figure 15: Design in 4Nec2

7.2 Strip discone antenna

We attempted to simulate the discone antenna in hopes that it would have similarities in performance with the biconical antenna [11] while satisfying size constraints. For this we used MATLAB's predefined antenna model and also made a wire model in 4Nec2. While the Bandwidth of the antenna was very() good, the gain of the antenna was fairly low and omnidirectional, which would have caused problems with isolating the antenna signals from noise. We tried to add reflectors at various angles to improve the radiation pattern but to no avail.

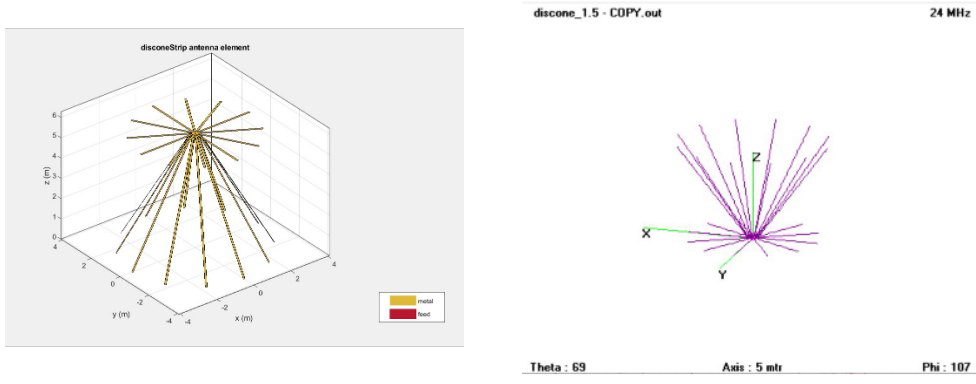


Figure 16: Matlab design

Figure 17: 4Nec2 Design

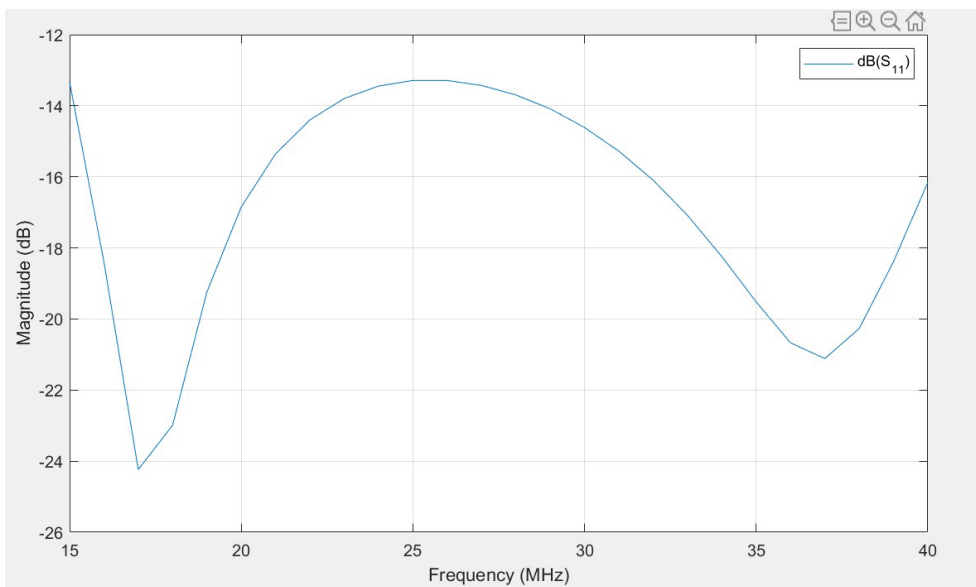


Figure 18: S11 for strip discone antenna

7.3 Bow-tie antenna

We attempted to design and simulate a modified bow-tie antenna using wire elements and a reflector sheet from 4nec2. The results were promising but the bandwidth (10 MHz in width) was less than that required by Guru Dhwani

objectives. 12

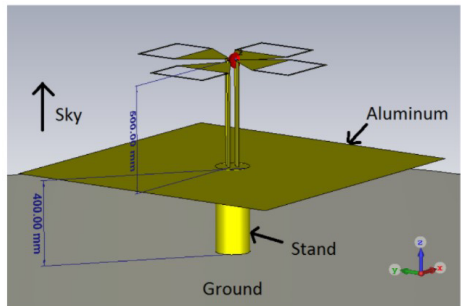


Figure 19: Original design

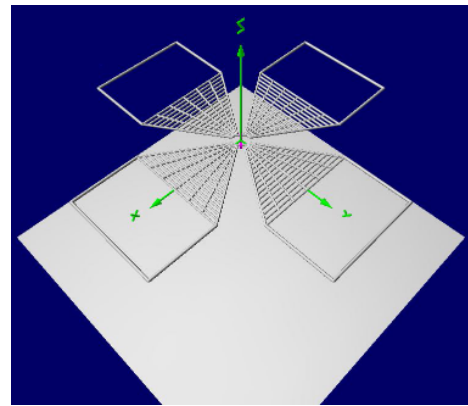


Figure 20: 4Nec2 Design

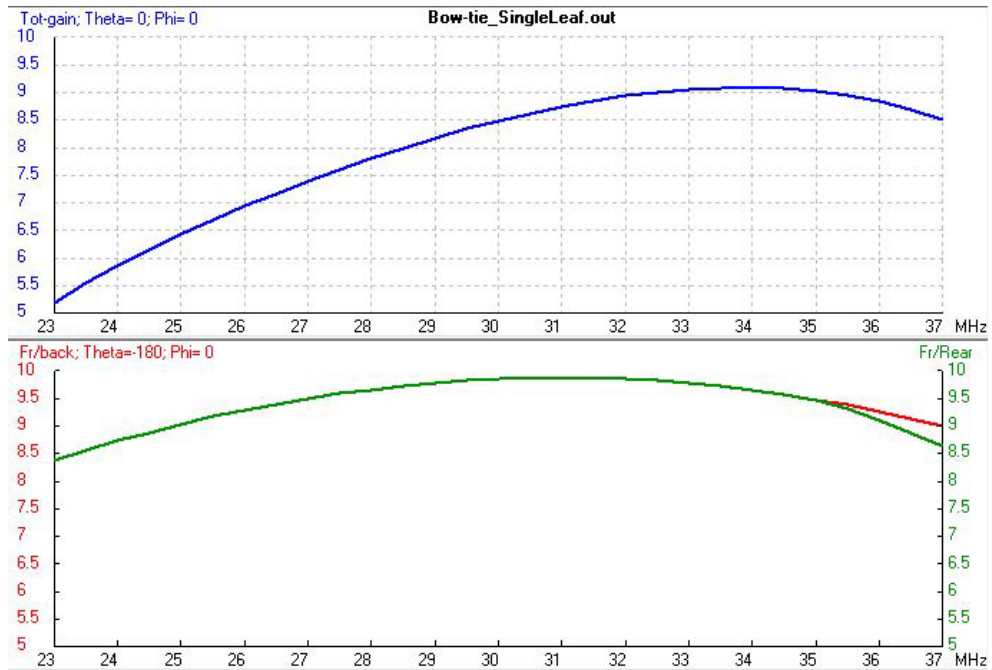


Figure 21: Gain and Fr/Back ratio

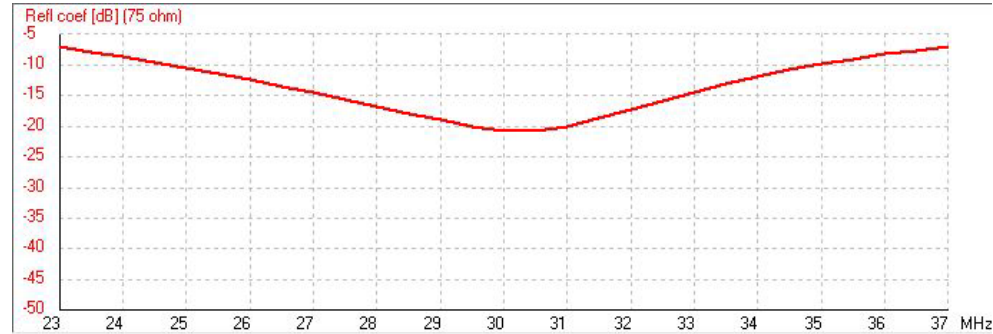


Figure 22: S11

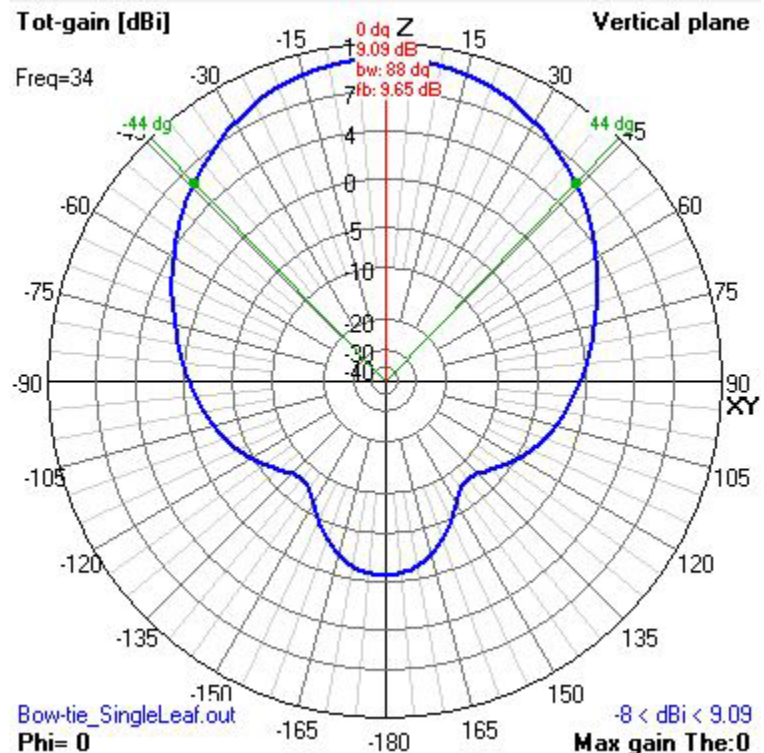


Figure 23: Total-gain pattern @ 34 MHz

7.4 Closely spaced Yagi Uda antenna

A novel Yagi Uda antenna was designed using closely spaced folded dipoles as driven and parasitic elements. The gain values were good but the bandwidth was very small (0.06 MHz).

7.5 3D shortened corner re ector

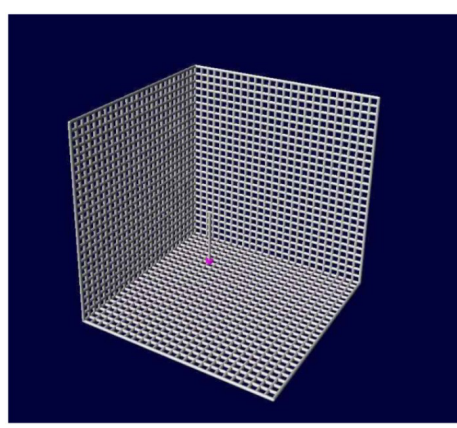


Figure 24: Original design

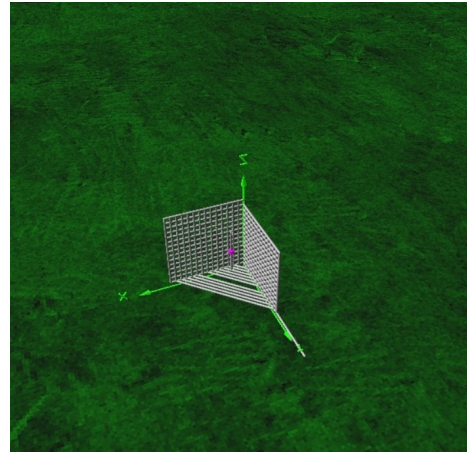


Figure 25: Team's Design

In this design adopted from [13] the length and spacing of the antenna and the length and the mesh spacing was altered. Although the gain was good near 20 MHz, the s11 was below -10 only near 36 MHz for a narrow bandwidth.

8 Acknowledgements

We would like to thank our mentor Prof.C.V.Krishnamurthy for excellent support, constant motivation and help with shortlisting designs and interpreting the results of simulations, this work would have been impossible without his backing. We would also like to thank our batchmates Aneesh Bhandari, Rohan Yadav and Harshita for their providing us assistance with 3D modeling,

9 Bibliography

We used the licensed version of Matlab and 4Nec2 for simulating various antenna systems.

1. CONSTRUCTION AND TESTING OF A 20.1MHz DIPOLE ARRAY [report](#)
2. Jovian decameter emissions observed by the Wind/WAVES radioastronomy experiment [link to the paper](#)
3. Dulk et.al 1994 [paper](#)
4. The Astrophysical Journal Supplement Series, 207:2 (5pp), 2013 July Raja et.al
5. IEEE TRANSACTIONS ON ELECTROMAGNETIC COMPATIBILITY, VOL. 41, NO. 2, MAY 1999
6. The Journal of Engineering doi: 10.1049/joe.2018.8392
7. ARRL Antenna Book 21st edition Chapter 10
8. Progress In Electromagnetics Research, PIER 72, 127–143, 2007
9. Receiving systems for radio astronomy Shubhendu Joardar
10. Handbook of Antenna Technologies [Paper](#)
11. R. Kudpik, K. Meksamoot, N. Siripon and S. Kosulvit, "Design of a compact biconical antenna for UWB applications," 2011 International Symposium on Intelligent Signal Processing and Communications Systems (ISPACS), 2011, pp. 1-6, doi: 10.1109/ISPACS.2011.6146212.
12. Tatomirescu, Alexandru, and Alina Badescu. 2020. "Wideband Dual-Polarized VHF Antenna for Space Observation Applications" Sensors 20, no. 15: 4351. <https://doi.org/10.3390/s20154351>
13. by L.B. Cebik W4RNL "The 3-D Corner Reflector" [link](#)